Journal of Engineering Science and Technology
Vol. 12, No. 4 (2017) 935 - 947

USING ONE-CYCLE CONTROL BASED SERIES VOLTAGE-SOURCED CONVERTER TO SUPPRESS STARTING CURRENT OF INDUCTION MOTORS

ALIREZA SADOUGHI[1], IMAN SADEGHKHANI[2,3,]*

[1]Department of Electrical Engineering, Malek-Ashtar University of Technology, Shahinshahr 115/83145, Iran
[2]Smart Microgrid Research Center, Najafabad Branch, Islamic Azad University, Najafabad 85141-43131, Iran
[3]Department of Electrical Engineering, Najafabad Branch, Islamic Azad University, Najafabad 85141-43131, Iran
*Corresponding Author: sadeghkhani@pel.iaun.ac.ir

Abstract

One of the most important concerns during Induction Motor (IM) starting is high starting current. This current can be 5 to 8 or more times the rated current. This phenomenon affects not only winding insulation but also power quality issues. The paper deals with a method of reducing the starting current. A Voltage-Sourced Converter (VSC) is connected in series to the IM and One-Cycle Control (OCC) is employed as switching technique. Since the series VSC acts as a dynamic resistor, starting current can be reduced effectively. The main principle of the proposed methodology is discussed. Also, symmetrical and asymmetrical Fault Ride-Through (FRT) capability of the induction motor using proposed method is investigated. The proposed technique is implemented using MATLAB/Simulink environment. Simulation results show the effectiveness of the proposed method for reduction of starting current and improvement of FRT capability.

Keywords: Induction motors, Voltage-sourced converter, One-cycle control, Starting current, Fault ride-through.

1. Introduction

The most common motor in various sections of the world including industrial, domestic, educational sections, etc. are induction motors [1-5]. Single-phase IMs are commonly used in the household applications, while three-phase ones are

Nomenclatures

C	Integrator capacitance, F
i_{motor}	Stator current, A
K_P	Proportional term, Ω
R	Integrator resistance, Ω
T_s	Switching period, s
V_{motor}	Voltage across the motor, V
V_{PCC}	PCC voltage, V
v_{out}	VSC output voltage, V
v_{ref}	VSC voltage reference, V

Abbreviations

DOL	Direct on-line
FRT	Fault ride-through
IM	Induction motor
OCC	One-cycle control
PCC	Point of common coupling
PWM	Pulse width modulation
THD	Total harmonic distortion
VSC	Voltage-sourced converter

widely used in the industry. The main advantages of this motor are its robustness, simple and rugged construction, reliability, low cost, little maintenance, wide range, high efficiency, reasonably good power factor, nearly constant speed, and self-starting torque [6]. However, these motors have some disadvantages such as difficult speed control, low power factor (lagging) in the lightly loaded condition, and high starting current.

One of the IM disturbances is the high starting current, also called inrush current, which can damage stator windings. Therefore, this current must be limited during starting period. The requirement for a starter is not only to provide starting but also to decrease high inrush currents and to provide overload and no-voltage protection. In the case of wound-rotor IM, the simplest and lowest cost method is to add a resistance to the rotor circuit through slip rings and brushes while nominal voltage is applied to the motor. The higher the rotor resistance, the less the starting current. On the other hand, some of the common methods employed to squirrel cage IMs are [7]: Direct On-Line starter (DOL), star-delta starter, autotransformer starter, stator impedance starter, power-electronics-based starter. DOL method is applied to the IMs less than 10 kW. In this approach, the IM is directly connected to the supply. Therefore, there is no reduction in the starting current. In the star-delta (Y-Δ) method, the IM is started in star connection, because in this condition the voltage across each phase is $1/\sqrt{3}\ V_{LL}$, where V_{LL} is line-to-line voltage. Thus, the IM takes 1/3 of the current from the supply when connected in star than when connected in delta. In the autotransformer starter, a partial of supply voltage is applied to the IM during starting period using an autotransformer. As a consequence, starting current is reduced. In the stator impedance starter, a resistance or a reactor is used in the stator circuit. During starting period, a portion of supply voltage is dropped across this impedance; thus starting current is decreased. Induction motor drive is a power-electronic-based tool for starting and control of IMs, which can reduce inrush current during IM starting.

In [8], by selection the proper torque reference, starting current of induction motors employed in the electric vehicles are reduced using Direct Torque Control (DTC). Magnetic Energy Recovery Switch (MERS) and magnetic retaining rings are used to decrease starting current of IMs in [9] and [10], respectively. Moreover, in [7] a parallel combination of resistors, self-inductors, and capacitors in the rotor circuit is proposed to reduce starting current of wound-rotor IMs. These methods are employed based on different requirements such as power supply capabilities, availability of equipment, sizing the network supply, installation cost, emergency capability and reliability of the system, etc. The first aim of selecting a method other than DOL is to decrease starting current or supply voltage of IM. As IM current is directly proportional to its voltage, reducing the voltage is very effective approach for starting current reduction [10-12].

This paper proposes a power-electronics-based approach to reduce starting current of IMs. A series voltage-sourced converter is employed for this purpose. One-cycle control technique is used to generate switching signals for VSCs. This approach introduces a dynamic resistance with respect to the stator current of IM, which results in reduction of starting current and improves fault ride-through capability of the induction motors. Several simulation results using MATLAB/Simulink are conducted to verify effectiveness of the proposed method.

The rest of paper is organized as follows. The proposed approach is introduced and analysed in Section 2. Simulation results are given in Section 3. Finally, Section 4 concludes this paper.

2. Proposed Methodology for Starting Current Reduction

2.1. Starting study

The Electric Motive Force (EMF) induced in the rotor depends on relative speed of rotor shaft and synchronous speed. Since in the starting condition the motor is standstill, this relative speed has its maximum value and therefore large EMF is induced in the rotor. When an induction motor is stationary, it behaves like a transformer which its secondary winding is short circuited. This causes low impedance to the system voltage and hence IM draws a high current from the gird, typically 5-10 times the full-load current. In some applications, this high current may cause a significant voltage drop in the power supply network affecting the operation of other equipment and also the motor start itself. In extreme cases, the power supply system may even shut down. Motor load doesn't affect starting current peak; although the inertia of the motor and load must be overcome. If inertia is big, the motor takes more time to reach full speed. When the motor accelerates, part of the starting current power overcomes this inertia and is converted to kinetic energy. The remaining power of the starting current heats the rotor, up to possibly 250^{o}C for a long starting (20 seconds).

The system considered for starting current study is shown in Fig. 1 in which the 3300 V network supplies two parallel loads including an induction motor and an R-L load at the Point of Common Coupling (PCC). The induction motor KHV355-2 from VALIADIS Company is considered in this paper. Parameters of this motor were calculated using no-load test, locked-rotor test, and DC test [13]. The electrical section of IM is represented by a fourth-order state-space model and the mechanical section by a second-order system [14]. Table 1 presents the parameters of test system. The motor is fully simulated in the MATLAB/Simulink. Figure 2 shows stator current of this motor for phase *a* in which the motor starts at t = 0.5 s; therefore this current is zero before 0.5 s. The starting current peaks for phase *a*, *b*, *c* are 266.5 A, 209.1 A, 213.5 A, respectively. The rated peak current of the studied motor is 58.9 A. Therefore, starting current in phase *a* is about 4.5 times the rated current. On the other hand, during starting period, a current with amplitude of 160 A (about 2 times the rated current) flows in the stator. As this starting period is relatively long for the large induction motors, thus these high currents should be limited. Proposed approach for this goal is presented in the next section.

Table 1. Test system parameters.

Parameter	Symbol	Value
Test Network		
Network voltage	V_q	3300 V
Fundamental frequency	f_g	50 Hz
Network resistance	R_q	0.4 Ω
Network reactance	X_g	0.63 Ω
Load resistance	R_L	100 Ω
Load reactance	X_L	31.42 Ω
Induction Motor		
Rated power	$P_{n\text{-}motor}$	200 kW
Rated voltage	$V_{n\text{-}motor}$	3300 V
Power factor	$cos\varphi$	0.84
Rated speed	N_n	2985 r.p.m
Stator resistance	R_s	0.65 Ω
Stator reactance	X_{ls}	5 Ω
Rotor resistance	R'_{lr}	0.65 Ω
Rotor reactance	X'_{lr}	5 Ω
Magnetizing reactance	X_m	113.82 Ω
Voltage-sourced converter		
Filter inductance	L_f	15 mH
Filter capacitance	C_f	150 μF
Switching frequency	f_s	5 kHz
DC link capacitor	C_{dc}	300 μF
Transformer		
Rated power	$S_{n\text{-}trans}$	5 kVA
Rated voltage	V_{Hn}/V_{Ln}	2.5/1.25 kV
High-voltage winding resistance	R_H	2.45 Ω
High-voltage winding reactance	X_H	62.83 Ω
Low-voltage winding resistance	R_L	0.61 Ω
Low-voltage winding reactance	X_L	15.39 Ω
Magnetization resistance	R_C	61347 Ω
Magnetization reactance	$X_{m,trans}$	195.27 Ω

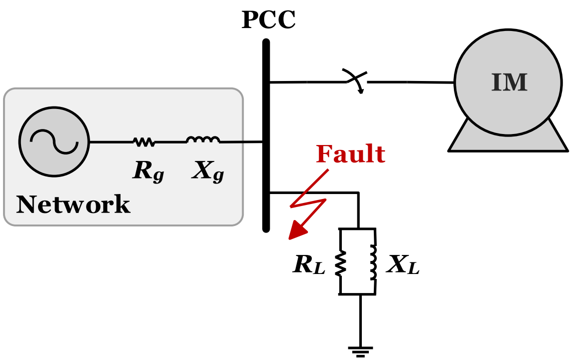

Fig. 1. Studied system for starting current evaluation.

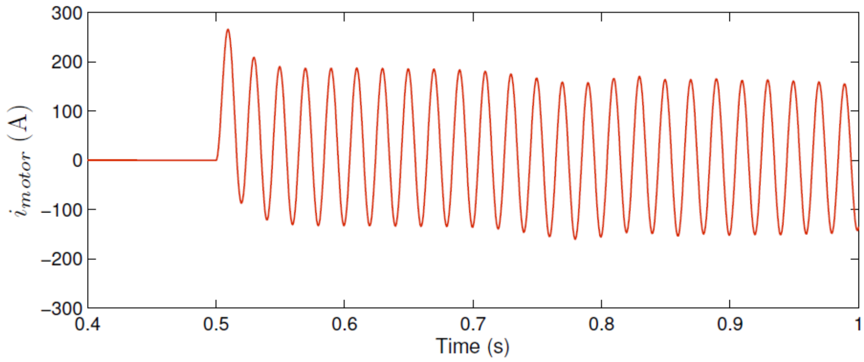

Fig. 2. Stator current of induction motor for phase *a* during starting.

2.2. Circuit topology

Application of the voltage-sourced converter in the induction motors and transformers has been already investigated in the literature [15-19]. This paper presents a series VSC to decrease the starting current. Figure 3 shows the proposed circuit for starting current reduction. Three VSCs are connected in series with the IM and power supply through three matching transformers. The proper passive (LC) filters are connected to the output side of the VSCs to limit switching ripples. In this work, three full-bridge, single-phase, two-level VSCs (or three H-bridge converters) are employed. The switching signals of VSCs are provided as follows. For simplicity, the proposed control scheme is implemented in the natural reference frame (*abc* coordinates), although the synchronous reference frame can also employed. First, input current to the motor (stator current) are measured and then multiplied by K_P [Ω] (proportional controller) to produce reference voltage for VSCs:

$$v_{ref}(t) = K_P \cdot i_{motor}(t) \tag{1}$$

where i_{motor} is the stator current. As mentioned in (1), the VSC voltages are in phase with the motor currents. Since the VSCs are connected in series to the connecting line, they act as the dynamic series resistors. Indeed, series VSC works as a dependent voltage source which its voltage is proportional with motor current, as shown in Fig. 4. Thus, in the starting period in which motor current is high, this dependent voltage source introduces a high voltage against the PCC voltage and therefore lower voltage appears across the motor terminal. Consequently, starting current is properly reduced. This operation can be expressed as:

$$\bar{V}_{motor} = \bar{V}_{PCC} - \left(K_P \times \bar{I}_{motor}\right) \tag{2}$$

where $\bar{V}_{motor}$ and $\bar{V}_{PCC}$ denote voltage across the motor and PCC voltage, respectively.

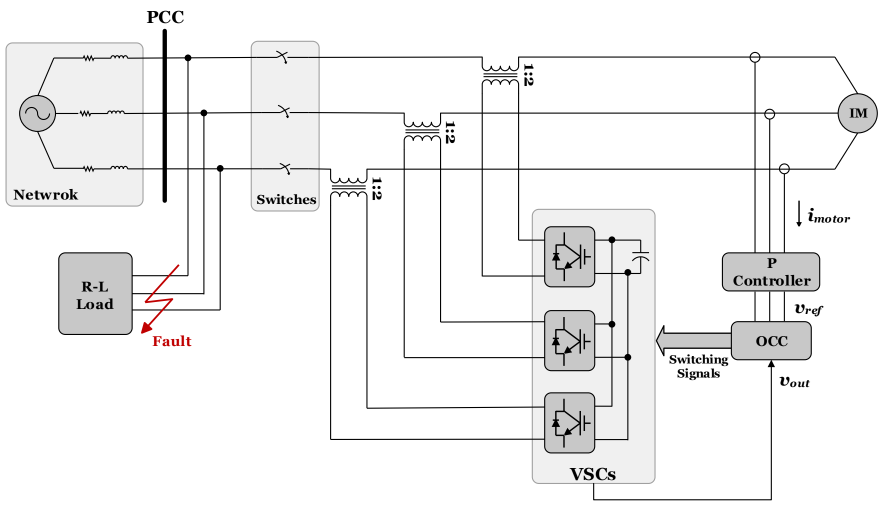

Fig. 3. Proposed control for starting current reduction.

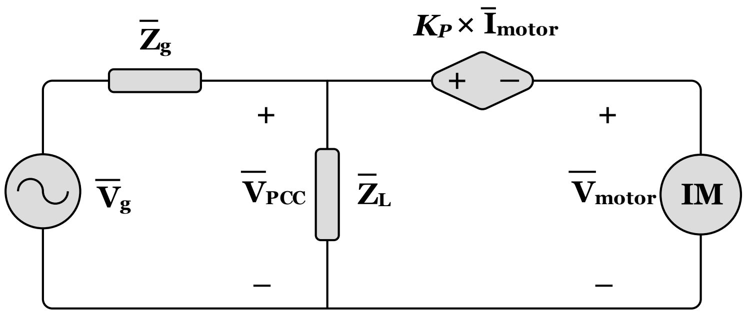

Fig. 4. Equivalent circuit of the studied system with proposed control.

2.3. One-cycle control

One-cycle control is a non-linear control method which not only presents fast transient response, good dynamic tracking performance, robustness, high power quality waveforms, etc. but also overcomes disadvantages of conventional Pulse Width Modulation (PWM) technique [20-22]. For this reasons, OCC technique is employed in this paper to provide switching signals of VSCs. The main core of

OCC is shown in Fig. 5. As shown in this figure, Clock block generates a periodic signal which sets the flip-flop at the beginning of each switching cycle. OCC receives two signals: (i) voltage reference produced by (1), and (ii) VSC output voltage. The output voltage of VSC is applied to the integrator as a feedback and compared with the voltage reference. When these signals meet, flip-flop is reset. This procedure is repeated in the next cycle for new voltage reference. This operation can be expressed as [23]:

$$v_{ref}(t) = \frac{1}{RC}\int_0^{dT_s} v_{out}(t)dt \tag{3}$$

where v_{out} is the output voltage of VSC, T_s is the switching period, and d (in dT_s) is the duty ratio. R and C are the resistance and capacitance of the integrator which T_s=RC.

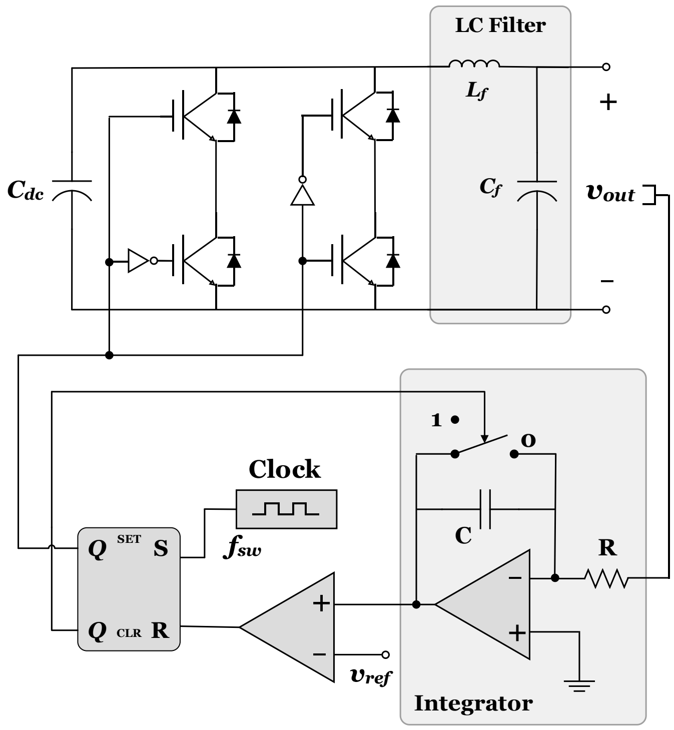

Fig. 5. Schematic diagram of OCC scheme.

3. Simulation Results

3.1. Starting performance

In this section, performance of the proposed control during starting period is investigated. For this purpose, the system of Fig. 3 is simulated with parameters of Table 1. In this paper K_P is set to 35.5×10^{-3} Ω. Stator current of IM are shown in Fig. 6. The starting current peaks for phases a, b, c are 111.7 A (1.9 times the rated current), 84.4 A (1.4 times the rated current), 88 A (1.5 times the rated current), respectively. In other words, the current peaks are reduced by 2.4 times, 2.5 times, and 2.4 times with respect to direct-connected IM (Fig. 1). Also in the starting period, a current with amplitude of about 62 A (about equal to the rated current) is flowed through the stator windings. Figure 7 shows the motor voltage for phase *a*. As mentioned above, series VSC reduces the voltage across the motor; however, subsequent to starting period, motor voltage is increased because the motor current and consequently voltage reference were reduced based on (1). The electromagnetic torque-motor speed curve obtained by the proposed method is shown in Fig. 8. It's clear that due to voltage reduction, starting period is increased with respect to direct-connected IM. Table 2 shows total harmonic distortion (THD) in PCC voltage and network current during and after IM starting which demonstrates the high quality of voltage and current waveforms in the proposed method. It's worth mentioning that to show both starting and normal operation periods in one figure, motor inertia was reduced in the simulation. Also, the transformers should be short circuited during normal operation, as done in [18], to avoid voltage drop across them.

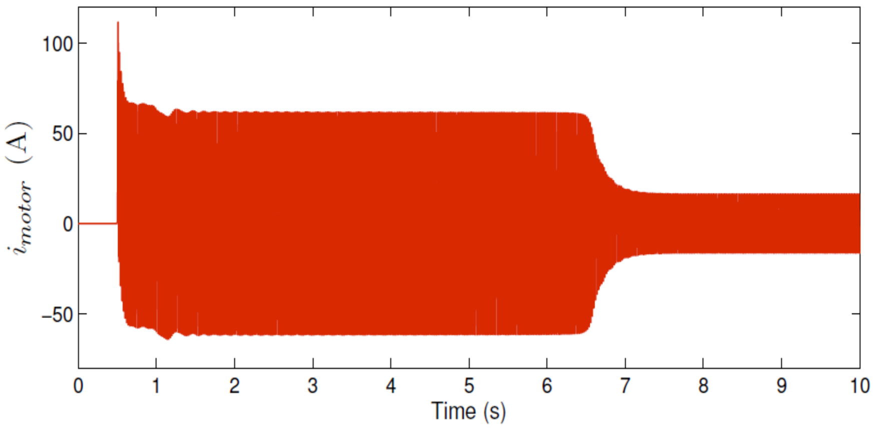

Fig. 6. Stator currents for phase *a* obtained by the proposed control.

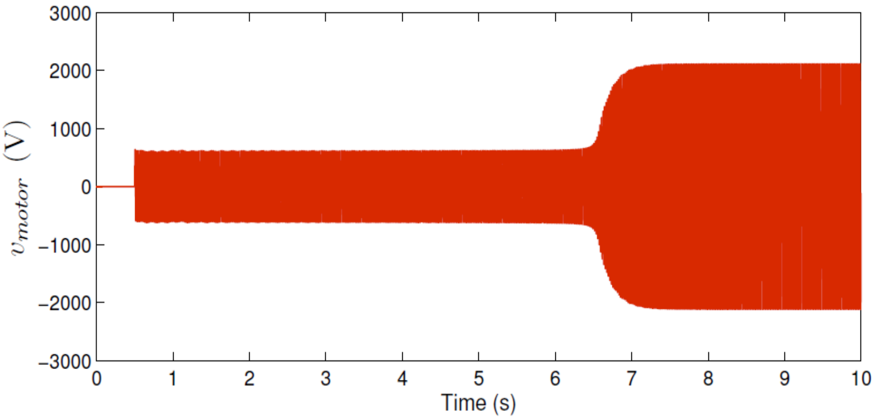

Fig. 7. Voltages across IM for phase *a* obtained by the proposed control.

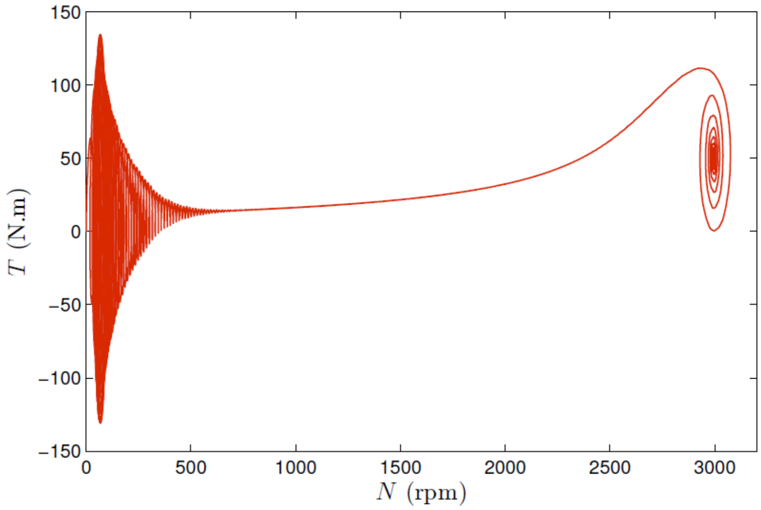

Fig. 8. Electromagnetic torque against motor speed obtained by the proposed control.

Table 2. Harmonic Analysis of Voltage and Current of the Network.

	During starting		Normal operation	
	THD_V (%)	**THD_I (%)**	**THD_V (%)**	**THD_I (%)**
Phase *a*	0.01	0.08	≈ 0	0.01
Phase *b*	0.01	0.17	≈ 0	0.03
Phase *c*	0.01	0.17	≈ 0	0.03

3.2. Fault ride-through performance

This section is dedicated to investigate fault behaviour of the proposed approach during both symmetrical and asymmetrical faults. First, the behaviour of the system of Fig. 1 during fault occurrence at the RL load terminal is studied. A three-phase to ground fault occurs at t = 8 s which lasts for 1 s. The fault resistance is 0.5 Ω. Simulation results are shown in Fig. 9. As shown in this figure, high currents are flowed during both fault inception and fault clearance. Also, a two-phase to ground fault is initiated at the load terminal. Figure 10 shows the stator currents in which high currents are flowed in the stator windings. Therefore, these high currents should be limited.

In the next stage, the fault behaviour of the proposed control is investigated during both symmetrical and asymmetrical faults. Simulation results for a three-phase to ground fault at the RL load terminal are shown in Fig. 11. Since the motor current is increased at the fault inception (Fig. 9), VSC provides a voltage proportional with this current to prevent flowing the high currents at the motor. On the other hand, as the PCC voltage and therefore voltage across the motor terminal are suddenly increased at the fault clearance, the motor current is again increased. Therefore, the above procedure is repeated and the motor current is limited. As shown in Fig. 11, the maximum peak current among all phases at the fault inception is 45.4 A which is decreased about 5.6 times with respect to Fig. 9, while this peak current at the fault clearance is 76.9 A. Finally, the behaviour of the proposed control against a two-phase to ground fault is shown in Fig. 12. In this condition, the maximum peak current at the fault occurrence is 41.4 A which is reduced about 5.3 times with respect to Fig. 10, whereas this peak current at the fault clearance is 50.9 A. One can conclude from the above results that the proposed control properly limits the motor current during both symmetrical and asymmetrical faults.

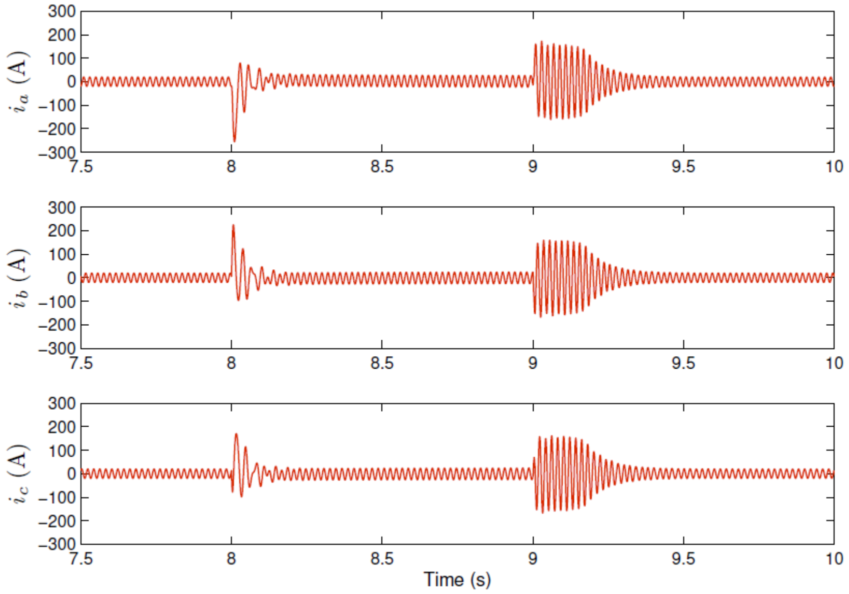

Fig. 9. Stator currents during an *a-b-c-g* fault.

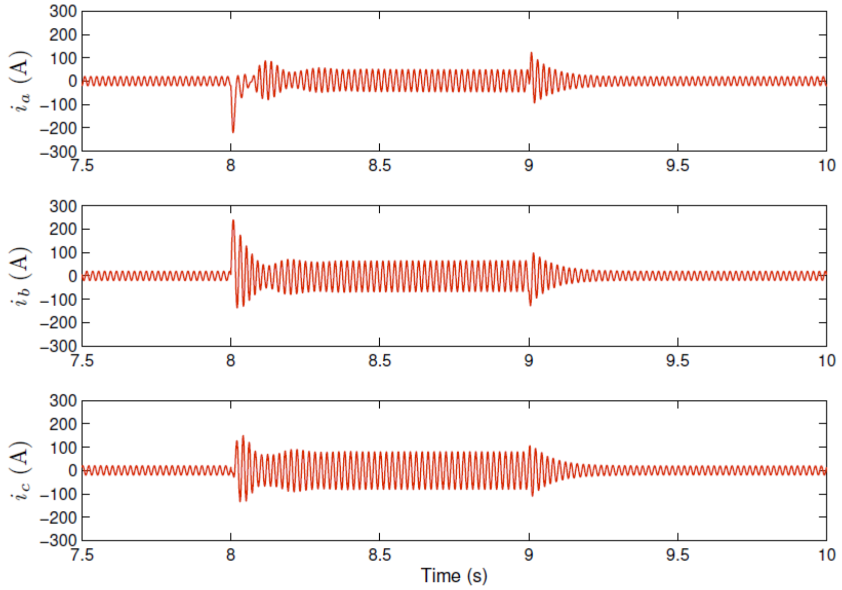

Fig. 10. Stator currents during an *a-b-g* fault.

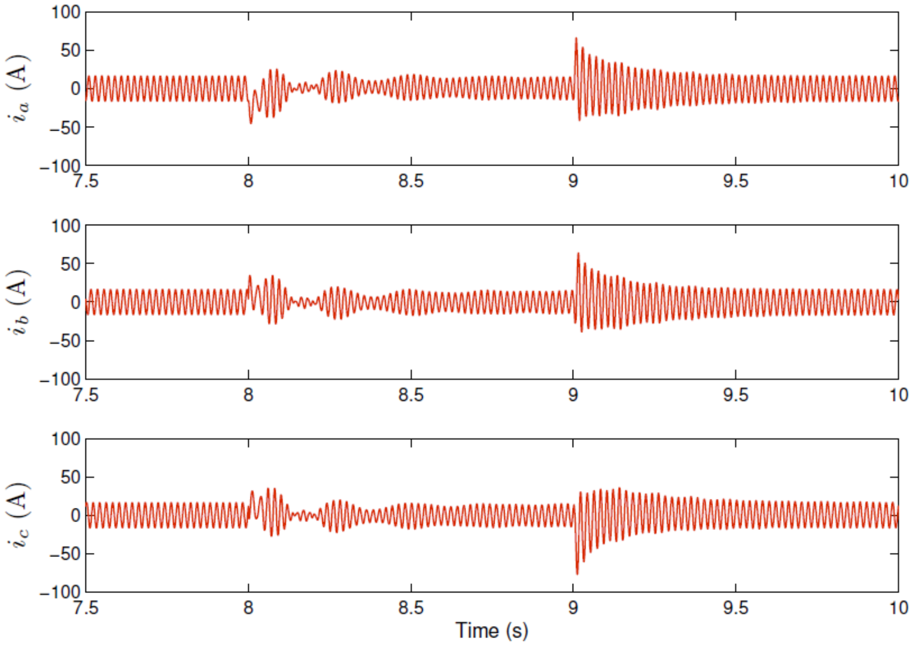

Fig. 11. Stator currents during an *a-b-c-g* fault obtained by the proposed control.

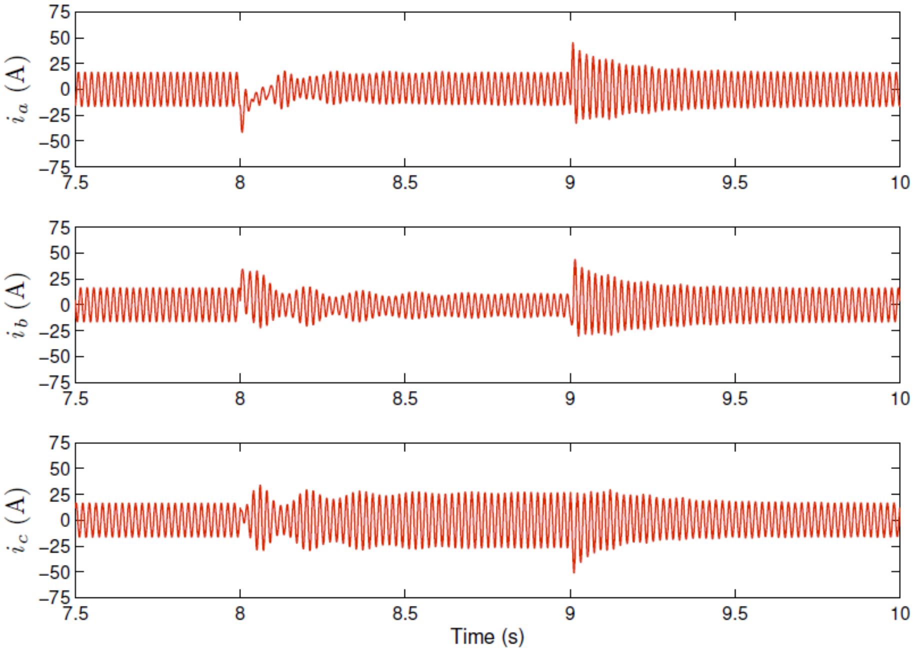

Fig. 12. Stator currents during an *a-b-g* fault obtained by the proposed control.

4. Conclusion

This paper proposes an effective approach to mitigate starting current of induction motors. A series voltage-sourced converter is employed for this purpose. Also, The OCC technique is used for generating switching signals of VSC. This method introduces a dynamic series resistance between source and motor which reduces the starting current. Simulation results show that starting current is reduced about 2.5 times with respect to direct-connected IM. Moreover, the study of the proposed control behaviour during both symmetrical and asymmetrical faults shows that the motor current is effectively reduced in these conditions (up to more than 5 times with respect to direct-connected IM) which verify fault ride-through capability of this control.

Acknowledgements

This work has been supported by the Iran's National Elites Foundation.

References

1. Lee, G.; Min, S.; and Hong, J.P. (2013). Optimal shape design of rotor slot in squirrel-cage induction motor considering torque characteristics. *IEEE Transactions on Magnetics*, 49(5), 2197-2200.
2. Ito, M.; Okuda, H.; Takahashi, N.; and Miyata, T. (1979). Starting current analysis of three-phase squirrel-cage induction motor by finite element method. *Electrical Engineering in Japan*, 99(1), 36-42.
3. Sivaraju, S.S.; Ferreira, F.J.T.E.; and Devarajan, N. (2012). Genetic algorithm based design optimization of a three-phase multiflux Induction Motor. *Proceedings of XXth International Conference on Electrical Machines (ICEM)*, Marseille, 288-294.
4. Buksnaitis, J. (2011). Analytical determination of mechanical characteristics of asynchronous motors by varying the electric current frequency. *Electronics and Electrical Engineering (Elektronika ir Elektrotechnika)*, 112(6), 3-6.
5. Vizhi, A.S.; Nagarajan, S.; and Ramareddy, S. (2012). Detection and analysis of broken bar in three phase squirrel cage induction motor using FEM. *Proceedings of International Conference on Computing, Electronics and Electrical Technologies (ICCEET)*, Kumaracoil, 40-50.
6. Sadoughi, A.; and Sadeghkhani, I. (2014). An intelligent estimator for transient overvoltages study during induction motors starting. *The Journal of Mathematics and Computer Science*, 9(4), 249-262.
7. harifian, M.; Feyzi, M.; Sabahi, M.; and Farrokhifar, M. (2011). A new soft starting method for wound-rotor induction motor. *Journal of Electrical Engineering*, 62(1), 31-36.
8. Zhu Hao; and Sun Xudong (2005). Starting current limitation method of DTC controlled induction machine for EV. *Proceedings of Eighth International Conference on Electrical Machines and Systems, ICEMS 2005*, 1, 836-838.
9. Danang Wijaya, F.; Kusumawan, S.A.; and Prabowo, H. (2014). Reducing induction motor starting current using magnetic energy recovery switch

(MERS). *Proceedings of 6th International Conference on Information Technology and Electrical Engineering (ICITEE).*

10. Portos, J.; King, R.; and Gaynor, P.A. (2009). The influence of magnetic retaining rings on ac motors for boosting torque and reducing starting current. *IEEE Transactions on Industry Applications*, 45(3), 1139-1145.
11. Bruce, F.M.; Graefe, R.J.; Lutz, A.; and Panlener, M.D. (1984). Reduced-voltage starting of squirrel-cage induction motors. *IEEE Transactions on Industry Applications*, IA-20(1), 46-55.
12. Larabee, J.; Pellegrino, B.; and Flick, B. (2005). Induction motor starting methods and issues. *Proceedings of 52nd Annual Petroleum and Chemical Industry Conference, Industry Applications Society*, 217-222.
13. Sen, P.C. (1997) *Principles of electric machines and power electronics* (2nd ed.). John Willey.
14. Krause, P.C.; Wasynczuk, O.; Sudhoff, S.D.; and Pekarek, S. (2013). *Analysis of electric machinery and drive systems* (3rd ed.). Wiley-IEEE Press.
15. Stumpf, P.; Varga, Z.; Kalman, R.J.; and Nagy, I. (2011). Analysis of space vector modulation techniques applied in voltage source converters of ultrahigh speed induction motor drives. *Proceedings of 14th European Conference on Power Electronics and Applications (EPE)*, Birmingham.
16. Pitic, C.I.; and Klumpner, C. (2008). A new matrix converter-voltage source converter hybrid arrangement for an adjustable speed-open winding induction motor drive with improved performance. *Proceedings of 4th IET Conference on Power Electronics, Machines and Drives, PEMD*, York, 60-65.
17. Jalili, K.; Malinowski, M.; and Bernet, S. (2005). Rotor flux oriented control of a high speed induction motor drive applying a two-level voltage source converter with LC-sine filter. *Proceedings of European Conference on Power Electronics and Applications*, Dresden.
18. Yamada, H.; Hiraki, E.; and Tanaka, T. (2006). A novel method of suppressing the inrush current of transformers using a series-connected voltage-source pwm converter. *Proceedings of International Conference on Power Electronics and Drives Systems, PEDS*, 1, 280-285.
19. Ketabi, A.; and Hadidi Zavareh, A.R. (2011). New method for inrush current mitigation using series voltage-source PWM converter for three phase transformer. *Proceedings of 2nd Power Electronics, Drive Systems and Technologies Conference (PEDSTC)*, Tehran, 501-506.
20. Li Xiangli; and Qi Hanhong (2012). One-cycle controlled single phase ups inverter. *Physics Procedia*, 25, 1048-1054.
21. Lihong He; Dexuan Zou; and Jianhua Wu (2008). Buck converter based on one-cycle control and PD control. *Proceedings of Chinese Control and Decision Conference, CCDC*, 3235-3238.
22. Yazdekhasti, A.; Ketabi, A.; and Sadeghkhani, I. (2015). One-cycle control application to wind turbine power control. *International Transactions on Electrical Energy Systems*, 25(10), 2427-2442.
23. Smedley, K. (2008). One-cycle controller for renewable energy conversion systems. *Proceedings of 34th Annual Conference of IEEE Industrial Electronics, IECON*, 13-16.